TOPOLOGICAL OPTICS

A fractional corner anomaly reveals higher-order topology

Christopher W. Peterson¹, Tianhe Li², Wladimir A. Benalcazar³, Taylor L. Hughes², Gaurav Bahl⁴*

Spectral measurements of boundary-localized topological modes are commonly used to identify topological insulators. For high-order insulators, these modes appear at boundaries of higher codimension, such as the corners of a two-dimensional material. Unfortunately, this spectroscopic approach is only viable if the energies of the topological modes lie within the bulk bandgap, which is not required for many topological crystalline insulators. The key topological feature in these insulators is instead fractional charge density arising from filled bulk bands, but measurements of such charge distributions have not been accessible to date. We experimentally measure boundary-localized fractional charge density in rotationally symmetric two-dimensional metamaterials and find one-fourth and one-third fractionalization. We then introduce a topological indicator that allows for the unambiguous identification of higher-order topology, even without in-gap states, and we demonstrate the associated higher-order bulk-boundary correspondence.

opological insulators (TIs) are materials with a gapped band structure characterized by quantized quantities, called topological invariants, that are invariant under deformations that preserve both the bulk bandgap and any protective symmetries (1, 2). At a boundary between two materials that have different strong topological invariants—i.e., where a topological invariant changes in space—the bandgap closes, and robust boundary-localized gapless modes appear. Detection of these robust gapless boundary modes is therefore one of the most striking signatures of topological materials.

We focus on two-dimensional (2D) TIs in class AI (spinless and time-reversal symmetric) (3). In this class and dimension, no nontrivial strong topological invariants exist (i.e., those protected by particle-hole, chiral, and/or time-reversal symmetry, such as the \mathbb{Z}_2 invariant for a quantum spin Hall insulator in class AII), but invariants can be defined if additional spatial symmetries are present. Materials with invariants protected by spatial symmetries are known as topological crystalline insulators (TCIs) (4, 5). We are specifically interested in a recently discovered class of TCIs whose members have gapped boundaries of codimension one but host gapless modes at boundaries with codimension greater than one, i.e., at a boundary of a boundary (6-9). Because these insulators manifest robust gapless modes at boundaries with higher codimension, they have been termed higher-order topological

waveguide arrays (17, 18), and photonic or sonic crystals (19–23). So far, the clearest indicator of higher-order topology in such systems has been the spectroscopic measurement of robust localized corner modes with energies inside the bulk bandgap of 2D (10–14, 17–23) and 3D (15, 16) HOTIs.

However, there is a fundamental problem with using localized in-gap boundary modes to identify higher-order topology (or, generally, topology protected by spatial symmetries). Spatial symmetries essentially divide a material

order gapless states.

However, there is a fundamental problem with using localized in-gap boundary modes to identify higher-order topology (or, generally, topology protected by spatial symmetries). Spatial symmetries essentially divide a material into symmetric sectors and require that localized modes in each sector are identical. Hence, these symmetries protect the degeneracy of boundary-localized modes but do not restrict their energy (24). Additional local symmetries (e.g., chiral symmetry or particle-hole symmetry) can pin the boundary modes to zero energy (midgap) (24, 25), but these symmetries are not actually necessary to protect the higherorder topology, and many lattice models do not support their implementation at all. This implies that the energy of localized boundary modes may reside either in the bulk gap or fully within the bulk bands of a HOTI, depending on the material's details. TIs that fall into the latter case do not host gapless boundary modes within their bulk bandgap and, as such, cannot be distinguished from trivial insulators by their spectrum alone, even with fully open boundary conditions.

insulators (HOTIs). We note that spatial sym-

metries are essential for these HOTIs because

they prevent bulk and surface deformations

that hybridize and gap out the set of higher-

Only a few naturally occurring HOTIs have

been identified (8, 9). Instead, much of the

experimental study of HOTIs (primarily d-th

order TCIs in d dimensions) has been per-

formed in engineered metamaterials, such

as networks of coupled resonators (10-16),

This fundamental principle means that HOTIs could be misidentified when their spectra do not exhibit in-gap modes, and it motivates the search for an experimentally measurable indicator of higher-order topology that is protected by only spatial symmetries. It has previously been established that spatial symmetries protect boundary-localized, quantized fractional charge in TCIs (6, 24, 26-29). In this work, we demonstrate that a similar feature in metamaterials-namely, the mode density of the spectral bands-can also be fractionally quantized and can diagnose both first-order and higher-order topology in gapped TCIs. In two dimensions, we term the quantity indicating second-order topology as a fractional corner anomaly (FCA) in the bulk mode density.

We define mode density as the local density of states (DOS) integrated over an entire band, which is equivalent to the charge density of a filled band in an electronic insulator. Unlike charge density, using mode density enables us to study the topology of bands without regard for electronic filling or constraints imposed by charge neutrality. In 2D TCIs, first-order nontrivial topology manifests as an edge-localized fractional mode density o. For TCIs with only first-order topology, the corner-localized fractional mode density ρ is the sum of the fractional mode densities, σ_1 and σ_2 , that respectively manifest at the edges that intersect to form that corner, such that $\rho = \sigma_1 + \sigma_2 \mod 1$ (modulo operation 1) (30). A fractional quantized deviation from this value definitively indicates higher-order topology, such that 2D TCIs without this deviation are not higherorder. To measure this type of higher-order feature in the bulk mode density, we define the FCA o, where

$$\phi = \rho - (\sigma_1 + \sigma_2) \bmod 1 \tag{1}$$

to capture second-order topology in 2D TCIs. A detailed motivation for the FCA and a generalized proof of this definition are provided in the supplementary materials (30).

Notably, although a nonzero FCA does not indicate that corner modes lie within the bulk bandgap, it does indicate the existence of robust topological corner modes somewhere in the spectrum-i.e., either within the bulk bands (or edge bands) or the bandgap. When topological corner modes are not spectrally isolated, the corner modes can generally couple to, and hybridize with, bulk or edge modes, although it was recently shown that in some cases corner modes within a bulk band can act as bound states in the continuum (31). However, when spectrally isolated from both the bulk and edge modes, they form the familiar exponentially localized 0D in-gap corner modes (10, 12, 13, 15, 16, 20). In the

¹Department of Electrical and Computer Engineering, University of Illinois at Urbana-Champaign, Urbana, IL, USA. ²Department of Physics and Institute for Condensed Matter Theory, University of Illinois at Urbana-Champaign, Urbana, IL, USA. ³Department of Physics, The Pennsylvania State University, University Park, PA, USA. ⁴Department of Mechanical Science and Engineering, University of Illinois at Urbana-Champaign, Urbana, IL, USA.

^{*}Corresponding author. Email: bahl@illinois.edu

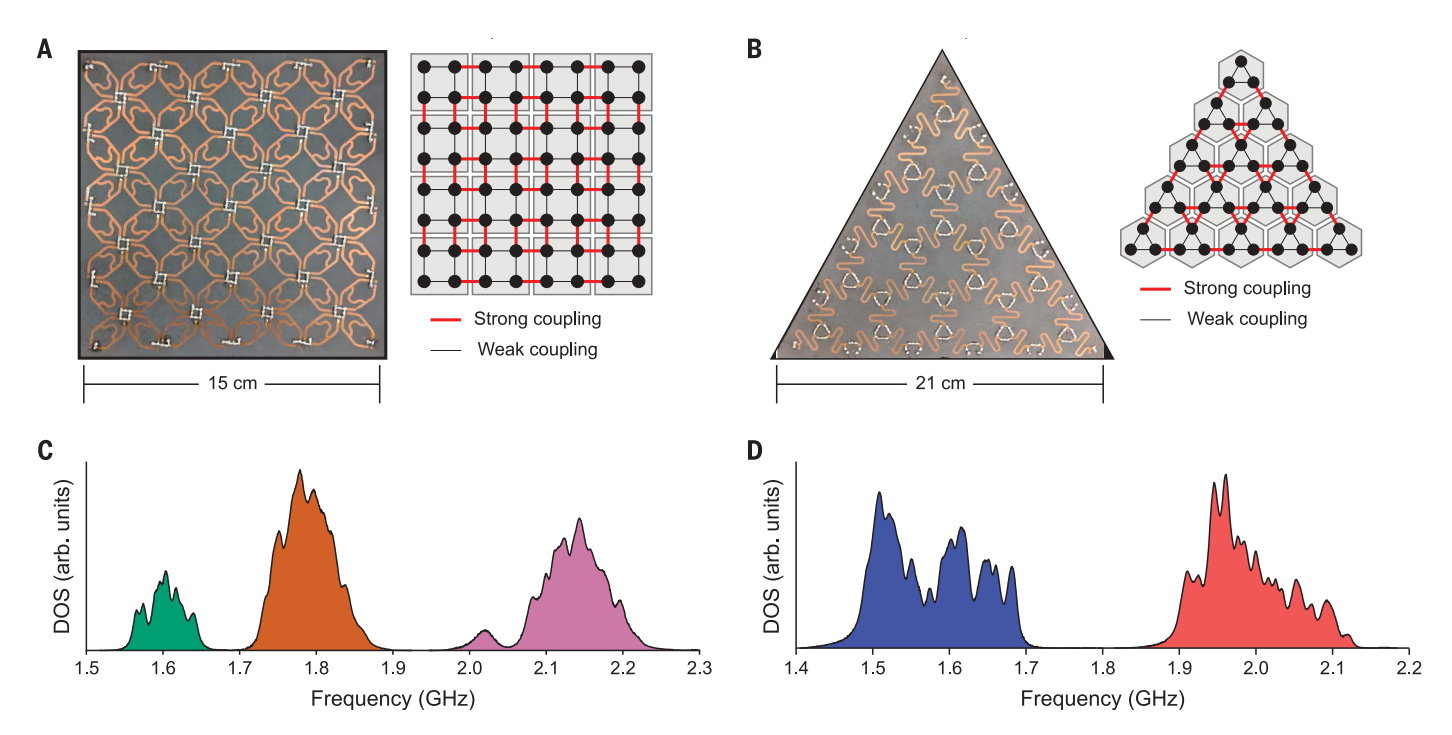


Fig. 1. Fabricated metamaterials and measured spectra. (**A**) Photograph of the experimental resonator array with C_4 symmetry. The schematic on the right illustrates the coupling between resonators. (**B**) Photograph of the experimental resonator array with C_3 symmetry. The schematic on the right illustrates the coupling between resonators. (**C**) Measured DOS spectrum for the resonator array in (A). arb. units, arbitrary units. (**D**) Measured DOS spectrum for the resonator array in (B).

next section, we experimentally measure a nonzero FCA in insulators where the corner modes are hybridized with bulk modes. Simulation results, detailed in the supplementary materials (30), show that the energy of topological corner modes can be tuned into, and even fully across, the bulk bandgaps (and any edge bandgaps) when a localized potential is applied to only the corner unit cells. We then demonstrate that these corner modes can be spectrally isolated and exponentially localized by deformation of the corner unit cell.

To observe the FCA experimentally, we constructed two rotationally symmetric TI metamaterials in microwave-frequency coupled resonator arrays. We chose to test two insulators with different symmetries because the quantization of the fractional mode density and FCA depends on the rotation symmetry group (24). The first insulator, shown in Fig. 1A, is on a square lattice with C_4 symmetry, and the second insulator, shown in Fig. 1B, is on a kagome lattice with C_3 symmetry. We first found the spectral DOS of both metamaterials by means of reflection measurements; see the supplementary materials (30) for details of the measurement technique. The measured spectrum of the C_4 -symmetric insulator, shown in Fig. 1C, has three distinct bands. The measured spectrum of the C_3 -symmetric insulator, shown in Fig. 1D, has two bands. Neither of these insulators have in-gap modes, so from the spectra alone it is not possible to tell whether either metamaterial is topologically nontrivial. However, as we will show, both are in fact nontrivial, and the intrinsic chiral symmetry breaking causes the edge and corner modes to lie within the bulk bands (30).

Next, we calculate the mode density of the measured bands by integrating the local DOS in each unit cell over their respective frequency ranges, as shown for both insulators in Fig. 2. The mode density of the C_4 -symmetric insulator is shown in Fig. 2A and has several important features on which we will focus. First, we find that the resonators in the bulk unit cells are excited in all three bands, which indicates that this insulator nominally has three bulk bands. We observe that the total mode density of these bands in each sector is approximately equal, which demonstrates that this insulator has approximate C_4 rotation symmetry with a small amount of symmetrybreaking disorder from fabrication imperfections. As expected, the mode density in the bulk unit cells, designated by $\mu^{(n)}$ (where the superscript indicates C_n symmetry), is always an integer. Specifically, $\mu_{1,3}^{(4)} \approx 1$ (where the subscript indicates the band number) and $\mu_2^{(4)} \approx 2$, which indicates that band 2 is a twofold degenerate band whereas bands 1 and 3 are nondegenerate.

Most importantly, we find a nonzero fractional mode density in the edge and corner unit cells. Because the bandgaps are relatively

large compared with the width of the bands (i.e., the system has a very short correlation length), the entirety of the fractional mode density is tightly localized within the boundary unit cells. For bands 1 and 3, the fractional mode density in the edge unit cells is $\sigma_{1,3}^{(4)} \approx \frac{1}{2}$, and in the corner unit cells it is $\rho_{1,3}^{(4)} \approx \frac{1}{4}$. In the twofold degenerate band 2, these fractions are doubled. This doubling occurs because band 2 is equivalent to two copies of band 1, in the sense that the Wannier representation of the orbitals in band 2 has two Wannier centers at Wyckoff position b, whereas band 1 has only one at position b(30); each Wannier center contributes equal fractional mode density to the boundary. The approximate fractions written above are obtained by rounding to the nearest quarter, as we anticipate that C_4 symmetry quantizes mode density in fractions of one-fourth (24).

We can now extract the FCA ϕ for each bulk band using the mode density data in Fig. 2A. Because the system is near a zero–correlation-length limit, we find ϕ using the simple formula $\phi = \rho - 2\sigma$, where ρ is the fractional mode density of the corner unit cell and σ is the fractional mode density of the edge unit cells (because of C_4 symmetry, all edges are expected to be identical). Here, because there is a small amount of unavoidable disorder in the experiment (which slightly breaks C_4 symmetry), we average over all the edges to find σ and over all the corners to find ρ ,

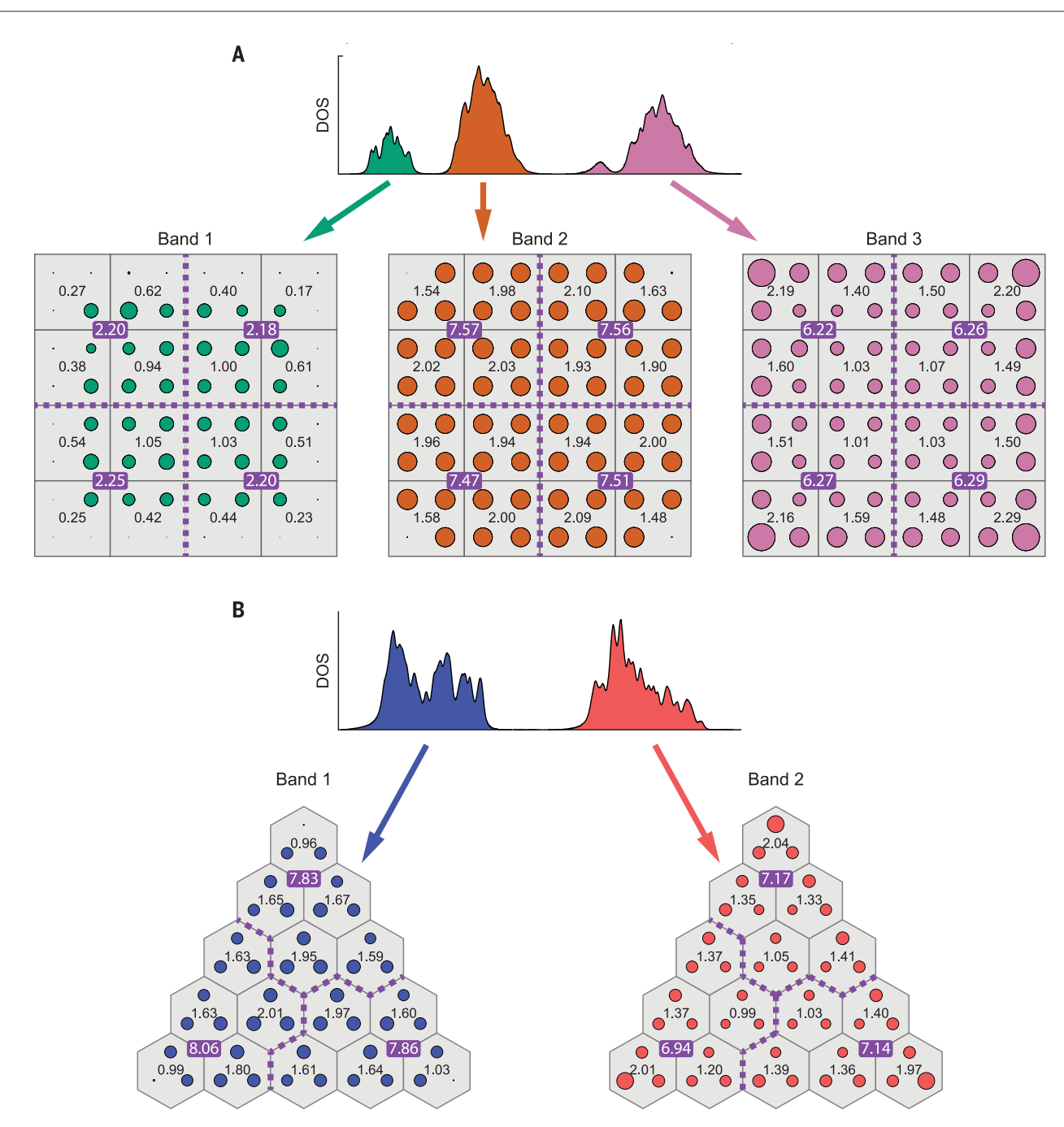


Fig. 2. Spatial distribution of bands. (**A**) Measured mode density for the C_4 -symmetric insulator. The mode density for each band is shown separately. Each filled circle represents a resonator, with the area of the circle corresponding to the measured mode density of that resonator in that band. The total mode density of each unit cell is shown with black text, and the total mode density of each sector is shown in purple with white text. (**B**) Same as (A) but for the C_3 -symmetric insulator.

such that $\phi_1^{(4)}-i.e.,$ the FCA for band 1 in the $C_4\text{-symmetric metamaterial}-is$

$$\phi_1^{(4)} = \rho_1^{(4)} - 2\sigma_1^{(4)} = 0.23 - 0.98$$

$$= 0.25 \approx \frac{1}{4}$$
(2)

A similar calculation can be carried out for the other bulk bands, giving $\phi_2^{(4)}=0.55\approx\frac{1}{2}$ for band 2 and $\phi_3^{(4)}=0.19\approx\frac{1}{4}$ for band 3. The sum of the FCA over all the bulk bands is always an integer (here rounding gives $\phi_1^{(4)}+$

$$\varphi_2^{(4)}+\varphi_3^{(4)}=0.99),$$
 and $\varphi_2^{(4)}$ is twice $\varphi_1^{(4)},$ as expected.

Next, we move on to the mode density for the C_3 -symmetric system, shown in Fig. 2B. For this material, we again find that the bulk unit cells have integer mode density, $\mu_1^{(3)} \approx 2$ (a twofold degenerate band) and $\mu_1^{(3)} \approx 1$. As in the previous system, the total mode density of these bands in each sector is approximately equal. The edge unit cells have a fractional mode density of $\sigma_1^{(3)} \approx \frac{2}{3}$ in band 1 and $\sigma_2^{(3)} \approx \frac{1}{3}$

in band 2. Here, the approximate fractions are obtained by rounding to the nearest third because this system is C_3 symmetric (24). Notably, although this material does not have a fractional mode density in the corner unit cells, the FCA indicator is nonzero, $\phi_1^{(3)}=0.70\approx\frac{2}{3}$, and $\phi_2^{(3)}=0.30\approx\frac{1}{3}$. For comparison, in the supplementary materials (30) we also present experimental measurements of the FCA for a trivial insulator and show that $\phi^{(3)}$, triv ≈ 0 for all bands.

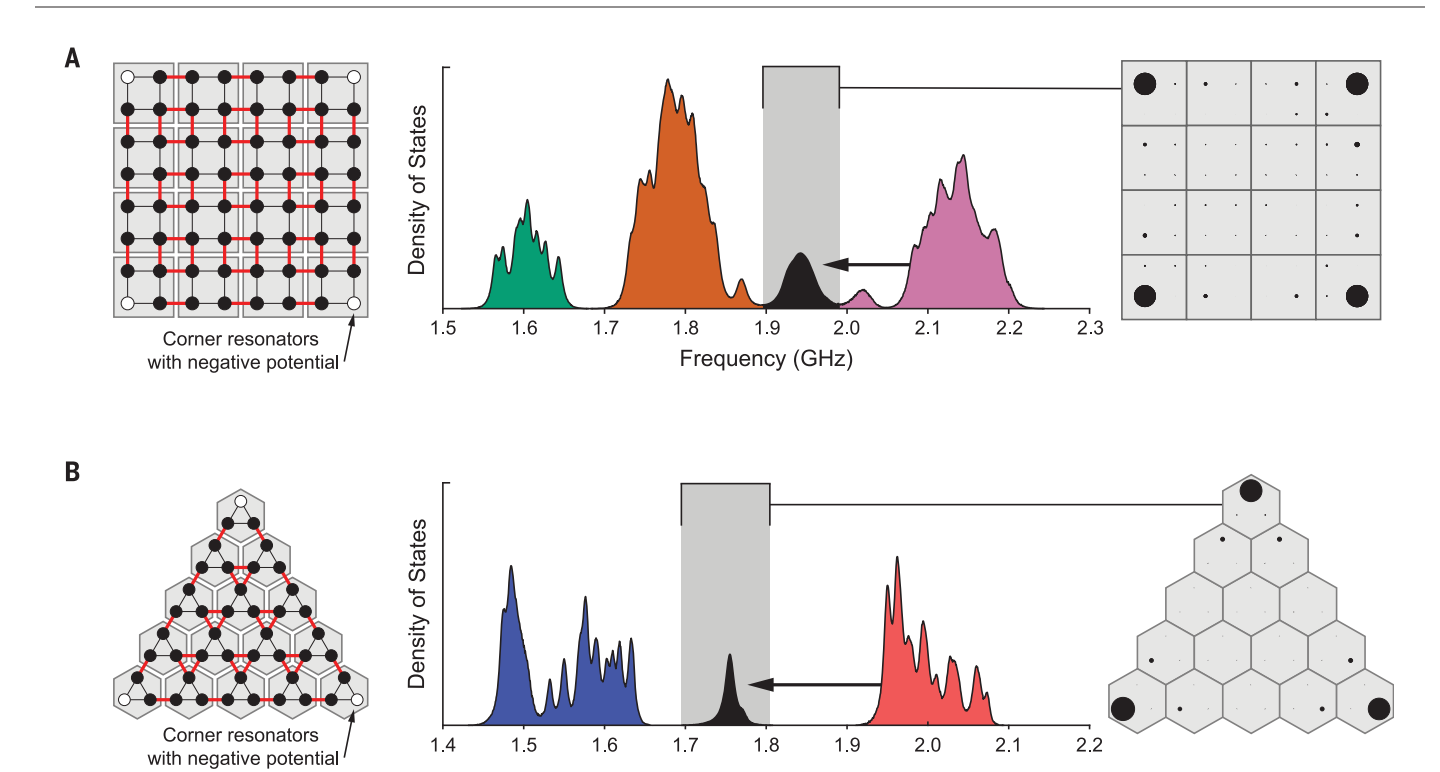


Fig. 3. Pulling topological modes into the gap. (A) The schematic on the left shows where a small, negative on-site potential is applied (white circles). The measured DOS has modes within the bulk bandgap, which are spatially localized to the corners and confined to one sublattice. (B) Same as (A) but for the C_3 -symmetric insulator.

Frequency (GHz)

The nonzero FCA in both metamaterials indicates that they are indeed HOTIs, and we have argued above that they should host second-order topological modes at their corners. Because we have not observed these expected topological modes within the bulk bandgap, we can estimate their spectral location by finding the band in which the corner resonators are most strongly excited. In the C_4 -symmetric system, the corner resonators, around which the second-order topological modes are expected to exist, are mainly excited in band 3, which indicates that the corner modes lie in this band. Moreover, this implies that we can spectrally localize these modes by slightly lowering the resonance frequency of the corner resonators. As illustrated in Fig. 3A, we applied a small negative potential to the corner resonators using a capacitor connected to ground, which decreases the electrical length (and thus the resonance frequency) of the corner resonators. When the potential is applied, we observe topological modes moving into the bandgap between bands 2 and 3 and becoming exponentially localized to the corner and confined to one sublattice.

In the C_3 -symmetric system, the corner resonators are only excited in band 2, which again indicates that the energy of the corner modes is too high and should be lowered to bring the modes into the bandgap. We pull these modes into the bandgap by similarly applying a small

negative potential to the corners, as illustrated in Fig. 3B. The topological modes are observed to spectrally localize within the bandgap and spatially localize to the corners with confinement on one sublattice. We also conducted a similar experiment on a trivial insulator (30) and found that localized corner modes cannot be isolated within the bulk bandgap, regardless of the applied potential strength.

The definition of the FCA can also be extended beyond two dimensions to identify d-th-order topology in fully gapped d-dimensional insulators. For example, the FCA for third-order TCIs in three dimensions is

$$\phi = \sum_{i,j} (\delta - \rho_j - \sigma_i) \bmod 1 \tag{3}$$

where δ is corner-localized fractional mode density, ρ_j is hinge-localized fractional mode density, and σ_i is surface-localized fractional mode density. Because this indicator captures fundamental topological features that are protected by spatial symmetries, we expect that it can assist with the experimental identification of materials with higher-order topology, which could otherwise be misidentified by only searching for in-gap corner modes. From a practical perspective, focusing on bulk-derived fractional mode density instead of localized modes could simplify experimental confirmations of novel TIs, which often use ad hoc supplementary boundary elements (e.g.,

auxiliary resonators or loading capacitors) to spectrally shift topological modes into the bandgap (22–25, 28, 29, 31).

REFERENCES AND NOTES

- 1. X.-L. Qi, S.-C. Zhang, Rev. Mod. Phys. 83, 1057-1110 (2011).
- M. Z. Hasan, C. L. Kane, Rev. Mod. Phys. 82, 3045–3067 (2010).
- A. P. Schnyder, S. Ryu, A. Furusaki, A. W. Ludwig, *Phys. Rev. B* 78, 195125 (2008).
- R.-J. Slager, A. Mesaros, V. Juričić, J. Zaanen, *Nat. Phys.* 9, 98–102 (2013).
- Y. Ando, L. Fu, Annu. Rev. Condens. Matter Phys. 6, 361–381 (2015).
 W. A. Benalcazar, B. A. Bernevig, T. L. Hughes, Science 357.
- W. A. Benalcazar, B. A. Bernevig, T. L. Hughes, Science 357 61–66 (2017).
- 7. Z. Song, Z. Fang, C. Fang, Phys. Rev. Lett. 119, 246402 (2017).
- 8. F. Schindler et al., Sci. Adv. 4, eaat0346 (2018).
- o. F. Schindler et al., Nat. Phys. 14, 918–924 (2018).
- C. W. Peterson, W. A. Benalcazar, T. L. Hughes, G. Bahl, Nature 555, 346–350 (2018).
- 11. S. Imhof et al., Nat. Phys. 14, 925–929 (2018).
- H. Xue, Y. Yang, F. Gao, Y. Chong, B. Zhang, *Nat. Mater.* 18, 108–112 (2019).
- X. Ni, M. Weiner, A. Alù, A. B. Khanikaev, *Nat. Mater.* 18, 113–120 (2019).
- 14. S. Mittal et al., Nat. Photonics 13, 692-696 (2019).
- 15. H. Xue et al., Phys. Rev. Lett. 122, 244301 (2019).
- M. Weiner, X. Ni, M. Li, A. Alù, A. B. Khanikaev, Sci. Adv. 6, eaay4166 (2020).
- 17. J. Noh et al., Nat. Photonics 12, 408-415 (2018)
- 18. A. El Hassan et al., Nat. Photonics 13, 697-700 (2019).
- 19. M. Serra-Garcia et al., Nature 555, 342-345 (2018).
- 20. X. Zhang et al., Nat. Phys. 15, 582–588 (2019).
- Z.-K. Lin, H.-X. Wang, Z. Xiong, M.-H. Lu, J.-H. Jiang, Nonsymmorphic Quadrupole Topological Insulators in Sonic Crystals. arXiv:1903.05997 [cond-mat.str-el] (14 March 2019).
- 22. B. Y. Xie et al., Phys. Rev. Lett. 122, 233903 (2019).
- 23. X. D. Chen et al., Phys. Rev. Lett. 122, 233902 (2019)
- W. A. Benalcazar, T. Li, T. L. Hughes, *Phys. Rev. B* 99, 245151 (2019).
- 25. J. Ahn, S. Park, B.-J. Yang, Phys. Rev. X 9, 021013 (2019).

- W. P. Su, J. R. Schrieffer, A. J. Heeger, *Phys. Rev. Lett.* 42, 1698–1701 (1979).
- 27. D. Vanderbilt, R. D. King-Smith, *Phys. Rev. B* **48**, 4442–4455 (1993).
- 28. R. Resta, Rev. Mod. Phys. 66, 899-915 (1994).
- 29. G. van Miert, C. Ortix, Phys. Rev. B 98, 081110 (2018).
- 30. Additional analyses are available as supplementary materials.
- W. A. Benalcazar, A. Cerjan, Bound states in the continuum of higher-order topological insulators. arXiv:1908.05687 [cond-mat.str-el] (15 August 2019).

ACKNOWLEDGMENTS

The authors would like to thank J. T. Bernhard for access to the resources at the University of Illinois at Urbana-Champaign Electromagnetics Laboratory, and they thank Q. Wang and W. Jiang

for assisting with the fabrication and measurement of the microwave circuits. **Funding:** This project was supported by the U.S. National Science Foundation (NSF) Emerging Frontiers in Research and Innovation (EFRI) grant EFMA-1627184. C.W.P. acknowledges support from the NSF Graduate Research Fellowship. G.B. acknowledges support from the U.S. Office of Naval Research (ONR) Director for Research Early Career Grant N00014-17-1-2209. T.L., W.A.B., and T.L.H. also thank the U.S. NSF under grant DMR-1351895. **Author contributions:** C.W.P. designed and fabricated the microwave circuits, performed the microwave simulations and experimental measurements, and produced the experimental figures. T.L. and W.A.B. guided the TI design and performed the theoretical calculations. T.L.H. and G.B. supervised all aspects of the project. All authors jointly wrote the paper.

Competing interests: The authors declare no competing interests. Data and materials availability: All data needed to evaluate the conclusions in the paper are present in the manuscript or the supplementary materials.

SUPPLEMENTARY MATERIALS

science.sciencemag.org/content/368/6495/1114/suppI/DC1 Materials and Methods Supplementary Text Figs. S1 to S4 References (32–45)

2 January 2020; accepted 14 April 2020 10.1126/science.aba7604



A fractional corner anomaly reveals higher-order topology

Christopher W. Peterson, Tianhe Li, Wladimir A. Benalcazar, Taylor L. Hughes and Gaurav Bahl

Science 368 (6495), 1114-1118. DOI: 10.1126/science.aba7604

Topological insulators in the spotlight

In addition to having an insulating interior while at the same time supporting conducting surface states, topological insulators have many other interesting properties. Higher-order topological insulating states, where regions of interest are along edges and at corners, have been difficult to identify unambiguously. Peterson et al. developed a theoretical framework to help identify and characterize these exotic states, including a new topological marker—the fractional charge density—that can be used to detect topological states of matter when the spectroscopic probe of gapless surface states is not accessible. The agreement between experimental work and theory is encouraging for applicability to other topological platforms.

Science, this issue p. 1114

ARTICLE TOOLS http://science.sciencemag.org/content/368/6495/1114

SUPPLEMENTARY http://science.sciencemag.org/content/suppl/2020/06/03/368.6495.1114.DC1

REFERENCES This article cites 43 articles, 3 of which you can access for free

http://science.sciencemag.org/content/368/6495/1114#BIBL

PERMISSIONS http://www.sciencemag.org/help/reprints-and-permissions

Use of this article is subject to the Terms of Service